Entropy-Driven Single Molecule Tug-of-War of DNA at Micro–Nanofluidic Interfaces

ARTICLE *in* NANO LETTERS · FEBRUARY 2012

Impact Factor: 13.59 · DOI: 10.1021/nl2045292 · Source: PubMed

4 AUTHORS, INCLUDING:

Jia-Wei Yeh
Cornell University
7 PUBLICATIONS **37** CITATIONS
SEE PROFILE

Alessandro Taloni
University of Milan
27 PUBLICATIONS **321** CITATIONS
SEE PROFILE

Yeng-Long Chen
Academia Sinica
68 PUBLICATIONS **1,095** CITATIONS
SEE PROFILE

NANO LETTERS

Letter

pubs.acs.org/NanoLett

Entropy-Driven Single Molecule Tug-of-War of DNA at Micro–Nanofluidic Interfaces

Jia-Wei Yeh,[†,‡,¶] Alessandro Taloni,[‡,#,¶] Yeng-Long Chen,[†,‡,⊥] and Chia-Fu Chou*[,‡,§,∥]

[†]Department of Physics, National Taiwan University, Taipei, Taiwan

[‡]Institute of Physics, [§]Research Center for Applied Sciences, and [∥]Genomics Research Center, Academia Sinica, Taipei, Taiwan

[⊥]Department of Chemical Engineering, National Tsing-Hua University, Hsinchu, Taiwan

Supporting Information

ABSTRACT: Entropy-driven polymer dynamics at the nanoscale is fundamentally important in biological systems but the dependence of the entropic force on the nanoconfinement remains elusive. Here, we established an entropy-driven single molecule tug-of-war (TOW) at two micro–nanofluidic interfaces bridged by a nanoslit, performed the force analysis from a modified wormlike chain in the TOW scenario and the entropic recoiling process, and determined the associated scalings on the nanoconfinement. Our results provide a direct experimental evidence that the entropic forces in these two regimes, though unequal, are essentially constant at defined slit heights, irrespective of the slit lengths and the DNA segments within. Our findings have the implications to polymer transport at the nanoscale, device design for single molecule analysis, and biotechnological applications.

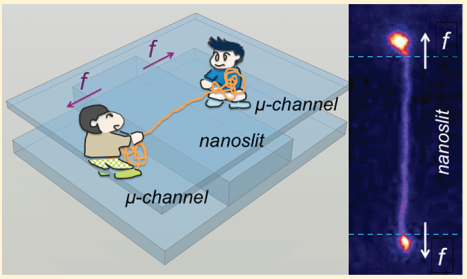

KEYWORDS: *Single molecule, tug-of-war, entropic force, nanofluidics, polymer dynamics*

In recent years, micro–nanofluidic interfaces have provided a playground for wide spectrum of fundamental studies and technical applications, ranging from the study of single polymer dynamics,[1−6] nanopore single molecule transport,[7−12] molecular separation and particle filtration,[13,14] to enhanced mass or charge transport at the nanoscale.[15−17] In particular, it serves an interesting motif to study entropy-driven molecular dynamics and transport at the nanoscale that is otherwise inaccessible at the microscale. One simple construct to study the entropy-driven phenomena of single biopolymers is to build a micro–nano interface, that is, an entropic barrier for biopolymers when the polymer's radius of gyration (R_g) is smaller than the height or width of a microfluidic channel but larger than that of a nanopore or a nanochannel.[18] In general, the nanoregion is entropically unfavorable for polymers due to the restricted conformational configurations caused by confinement. Nevertheless, polymers may be driven into the region with an external field.[2,6] Given a number of theoretical and experimental investigations on polymer systems under nanoconfinement, it remains elusive as to how the force, or the free energy change, scales on the degree of confinement that affect the polymer dynamics in nanoslit.[4,5,9,18−31] In this Letter, we construct two symmetric micro–nano interfaces bridged by a nanoslit to establish an entropy-driven single molecule tug-of-war (TOW) scheme which enables us to study the statics of DNA TOW and the dynamics of entropic recoiling under strong confinement (slit height h < Kuhn length, that is, ∼120 nm) to obtain the forces involved in these processes and the scaling on the degree of confinement. To our knowledge, this is the only system capable of studying both force–extension relation and the scaling under strong confinement, which is purely entropy-driven as occurs in many natural processes, without externally applied force through a sophisticated apparatus, such as an optical tweezers, magnetic tweezers, and atomic force microscopy as in previous studies.[9,32−34]

The basic design of the entropy-driven single DNA molecule TOW at the micro–nanofluidic interfaces is simple and illustrated in Figure 1a,e,f. The conformational entropy difference between a polymer chain confined in the nanoslit and in the microchannels induces equal and opposite entropic recoiling forces, f_{rec}, at the two micro–nano interfaces. This entropic force stretches the DNA segment inside the nanoslit, thereby establishing a TOW between the two random coils on the same DNA polymer across the nanoslit. When the entropically stabilized scenario ends, the chain quickly exits the nanoregion through a two-step process: elastic retraction, when the stretched molecule undergoes a rapid contraction (due to the force f_{el}) toward its equilibrium 2D configuration in the slit, and entropic recoiling, when the DNA coils out of the nanoslit into one of the microregions (i.e., transition from equilibrium 2D configuration in the slit to equilibrium 3D configuration in the microchannel), as shown in Figures 1b,g,i.[35] The advantage of this setup is that the initial withdrawal of DNA after TOW (t_0) and the distance of withdrawal (slit length) are well-defined, making it possible to study the scaling dependence that was previously inaccessible.[35]

Received: December 23, 2011
Revised: February 7, 2012
Published: February 13, 2012

   dx.doi.org/10.1021/nl2045292 | *Nano Lett.* 2012, 12, 1597−1602

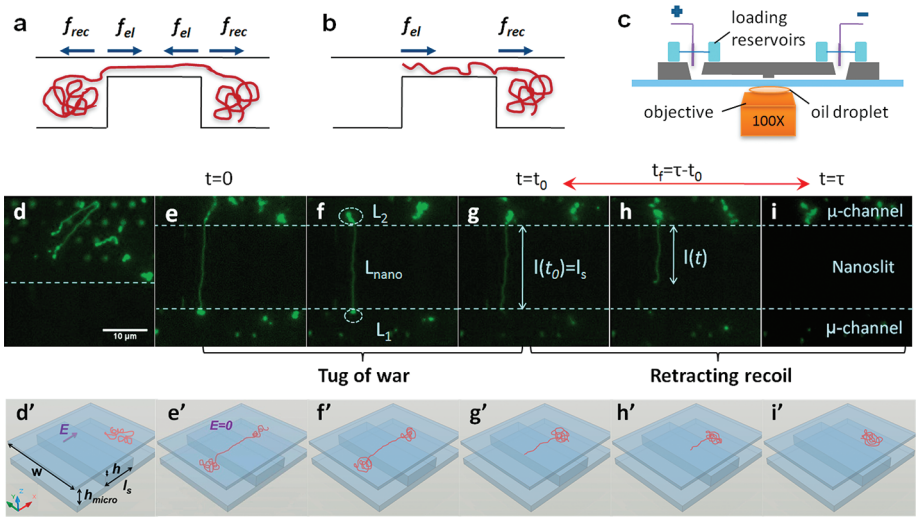

Figure 1. Single molecule TOW and the entropic recoiling of DNA at micro−nanofluidic interfaces. (a) Cross-sectional schematic of DNA TOW established by entropic recoiling force at two symmetric micro−nano interfaces. (b) Elastic recoiling of a single DNA from one microchannel to the other at the end of TOW. (c) Side view of the device and imaging setup. (d−i) Experimental procedures; the dashed lines are the interfaces between nanoslit and microchannels. (d) DNA is prestretched by pillars in microchannel and driven across the nanoslit (h = 50 nm) by a 0.8 V/cm electric pulse. (e) As one end of DNA reaches the other side of the nanoslit, it forms a TOW scenario when field is off. (f) DNA TOW may last from seconds to minutes (here L_1, L_2, L_{nano} are the contour length of DNA in two microchannels and in nanoslit, respectively). (g) Elastic retraction occurs in the nanoslit at $t = t_0$ when the TOW ends. The projected length $l(t_0)$ equals to the slit length l_s. (h) DNA starts entropic recoiling from the nanoslit back to the microchannel. (i) DNA retracts completely out of the nanoslit. (d′−i′) The 3D rendering of the corresponding process in (d−i).

The devices were fabricated through a differential etching process to define the nanoslits with length l_s from 4 to 30 μm, height h = 40, 50, 65, and 110 nm, and width w = 10 μm and the microchannels with height h_{micro} = 1.5 μm, as shown in Figure 1d′. Appropriate bonding techniques were employed for sealing the device with fluidic inlets and outlets.[36,37] The system setup is shown in Figure 1c (see Methods in Supporting Information). The entire TOW and exit process of bacteriophage T4 DNA (Wako, Japan), 166 kbp, stained with the SYBR-Gold fluorescent dye, was recorded (Figure 1d−i). In particular, the x−y plane-projected contour length of a DNA strand inside the nanoslit (L_{nano}) and its projected length $l(t)$ along the slit axis for various h and l_s were measured (Figure 1d′). Corrections to the planar (x−y) detected value of L_{nano}, including the vertical (z) fluctuations of the DNA molecule, were achieved by weighting the strand's contour by its intensity (see Supporting Information). The 3D rendering of the corresponding process is depicted in Figure 1d′−i′. Brownian dynamics (BD) simulations of semiflexible chains were also performed to determine the functional expression of the restoring elastic force f_{el} for nano-confined stretched polymers.

From our observations, the dynamics of a confined polymer crossing two micro−nano interfaces can be divided into two distinct regimes: TOW and retracting-recoiling. In the TOW regime, the polymer is entropically trapped within the nanoslit and assumed to be in quasi-equilibrium. The requirement is that the trapping time t_0 (Figure 1g) is much longer than the conformational equilibration time of a polymer.[38,39] In this state, the confinement-induced entropic force that "acts" to pull the DNA out of the nanoslit (f_{rec}) is counter-balanced at the micro−nano interfaces by the entropic elasticity of the stretched DNA strand inside the nanoslit (f_{el}) (Figure 1a and Supporting Information eq S6). Polymer theory from both the Odijk ($P > h$, with P the persistent length of the molecule)[20,21] and de Gennes ($P \ll h$) regimes,[19] suggests that f_{rec} is independent of the average contour length $\langle L_{nano}\rangle$ and on the slit length l_s, and it is only influenced by the degree of confinement h.

In the TOW regime, the analysis in Supporting Information (I) shows that $f_{rec} = -f_{el}(l_s)$, where f_{el} is the elastic restoring force on a confined polymer elongated to an end-to-end extension of l_s. The elastic force of the elongated polymer f_{el} may be determined from the wormlike chain (WLC) force−extension relation.[40] However, the WLC relation strictly applies for an unconfined long semiflexible chain with infinitesimal equilibrium extension. A modified WLC (mWLC) applicable for DNA in nanoslits, where the equilibrium extension l_{rel} is non-negligible, needs to take into account the confinement effects on the chain rigidity and the small and large elongation behavior. At small extension, the elastic force is linearly dependent on the deviation from equilibrium ($l - l_{rel}$). At high extension, the elastic force must recover the WLC form. BD simulations are performed to capture the mWLC force−extension relation, which turns out to be

$$f_{el} \cong \frac{k_B T}{l_c}\left[\frac{1}{4}\left(\frac{1}{(1-x)^2} - \frac{1}{(1-x_{rel})^2}\right) + (x - x_{rel})\right] \quad (1)$$

where $k_B T$ is the thermal energy, $x = l/\langle L_{nano}\rangle$ (at equilibrium, $x_{rel} = l_{rel}/\langle L_{nano}\rangle$) and l_c is the DNA segmental correlation length in the elongated dimensions,[41] a modified definition of the free DNA persistence length in nanoconfinement (see Supporting Information II). The BD results allow direct determination of l_c for different slit heights (Figure 2a inset). By setting $x = x_s \equiv l_s/\langle L_{nano}\rangle$ in eq 1, the entropic force pulling on the DNA strands at the micro−nano interface may be determined from Supporting Information eq S6. Since we expect that f_{rec} is independent of l_s and $\langle L_{nano}\rangle$, x_s must be constant for a given h. Indeed, Figure 2b shows the experimentally observed values of $\langle L_{nano}\rangle/l_s$= 1.13 ± 0.03, 1.17 ± 0.01, 1.19 ± 0.08, and 1.32 ± 0.03 (s.e.m.) for h = 40, 50, 65, and 110 nm slits, respectively. From the mWLC

dx.doi.org/10.1021/nl2045292 | Nano Lett. 2012, 12, 1597−1602

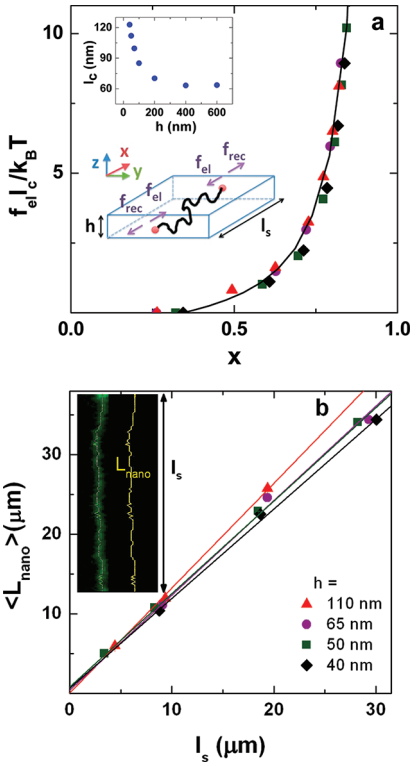

Figure 2. Tug-of-war phase. (a) The force–extension curve of semiflexible chains in nanoslits for h = 40 (black diamond), 50 (green square), 65 (brown inverse triangle), and 110 nm (red triangle) studied by Brownian dynamics simulation; schematic representation of the simulated system. Equation 1 is shown as the solid black line. The inset shows the segmental correlation length l_c (blue circle) in the unconfined direction as a function of h. The values of l_c (123, 112, 100, and 81 nm) are then used to determine f_{rec} from eq 1 for h = 40, 50, 65, and 110 nm, respectively (see Supporting Information Table S1). (b) The averaged contour length $\langle L_{nano}\rangle$ versus slit length l_s for h = 40, 50, 65, and 110 nm. The solid lines represent the corresponding linear fits of $\langle L_{nano}\rangle = l_s/x_s$, yielding $1/x_s$ = 1.13 ± 0.03, 1.17 ± 0.01, 1.19 ± 0.08, and 1.32 ± 0.03 (s.e.m.), respectively. (Inset) Typical case of DNA segments inside the nanoslit during the TOW phase; L_{nano} is tracked by imaging analysis (see Methods in Supporting Information).

expression (1), these values give the corresponding recoiling forces $|f_{rec}| \equiv |f_{el}(x_s)|$ = 0.51 ± 0.03, 0.35 ± 0.02, 0.33 ± 0.02, and 0.17 ± 0.01 (s.d.) pN (Supporting Information Table S1 and Figure 4b). To be noted, for h > 200 nm, the entropic force outside the nanoslit is not strong enough to stretch DNA, thus DNA relaxation length (l_{rel}) shorter than slit length makes it hard to form a TOW scenario. For small h (<25 nm), surface interactions may be much stronger than the forces due to the entropic confinement and the chain stretching cannot be simply described by entropic confinement presented in this work, hence it is not included in the discussion here. It is noted that seemingly the outlined TOW phase is similar to ref 6, where a slit-confined DNA extends across two (or more) etched nanopits. An important difference is that the nanopits in the previous study have depth of 200 nm, which is much smaller than R_g, whereas the microregion used here have depth of 1.5 μm, which is comparable to R_g. Thus, the free energy difference is much larger in the current system that helps stabilize the TOW scenario. On the other hand, the nanopit device is more suitable to explore the segmental fluctuation or jumping of a DNA where the DNA segments are not in the stable entropic energy landscapes. Further, the free energy of the slit-confined portion of a DNA was inferred from the bulk WLC force–extension relation in the nanopit device. Our study indicates that in nanoslits with height comparable to the DNA persistence length the segmental correlation length is strongly affected by the confinement, and a modified force–extension relation is more appropriate.

Near the end of the tug-of-war, one end of the chain translocates into the nanoslit, and the DNA molecule exits the nanoslit by entropic recoiling and retraction from $t = t_0$ (Figure 1g) to $t = \tau$ (Figure 1i) (retracting–recoiling dynamics). The projected length $l(t)$ of DNA along the slit axis is measured (Figure 3a inset). Each individual retracting

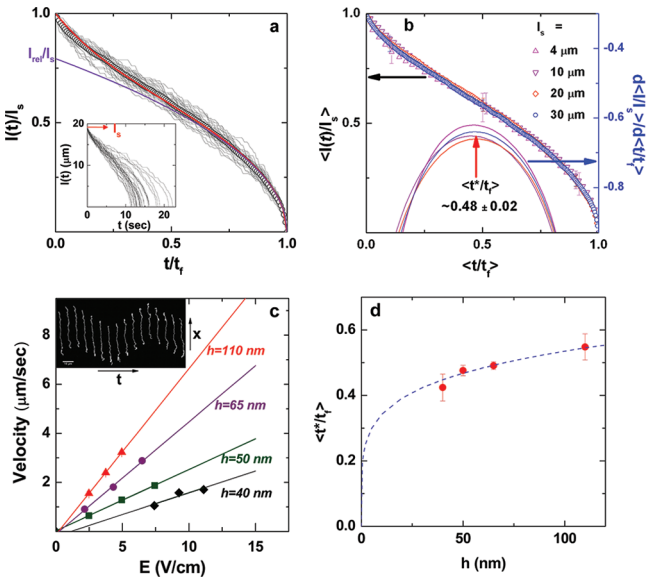

Figure 3. Retracting–recoiling phase. (a) Rescaled retracting–recoiling trajectories $l(t)$ of 40 molecules for slit length l_s = 20 μm and h = 50 nm. Each template's $l(t)$ (gray traces) has been rescaled by l_s, and t by the corresponding t_f. The averaged curve (○) was fitted with eq 3 (red line). The purple line indicates the purely entropic recoiling $l_{rec}(t)$: $l_{rec}(t)/l_s = B(1 - \langle t/t_f\rangle)^{1/2}$, with $B = l_{rec}(0)/l_s = l_{rel}/l_s$.[35] (Inset) Typical $l(t)$ before rescaling, the time origin of each trajectory t_0 has been shifted to 0. (b) Universal behavior of the rescaled curves and its first derivatives of the fitted retraction curves (solid lines), $d\langle l(t)/l_s\rangle/d\langle t/t_f\rangle$ for different l_s at h = 50 nm. The error bars for each l_s are shown only for $\langle t/t_f\rangle$ = 0.1, 0.5, and 0.9 for easy viewing. (c) Mobility measurements of DNA inside the nanoslit. The linear fits (solid lines) of the strand velocity versus the applied field yield μ = 0.18 ± 0.06, 0.25 ± 0.01, 0.46 ± 0.02, and 0.68 ± 0.04 (s.e.m.) × 10^{-4} cm^2/V·sec for h = 40, 50, 65, and 110 nm, respectively. Inset shows typical trajectories of a DNA molecule in the nanoslit when an alternating field was applied (square wave of ±200 mV/cm at 30 mHz) after the molecule was transported into the slit and relaxed to its equilibrium length (l_{rel}). The time interval between each frame is 5.2 s and the scale bar 10 μm. (d) Averaged retraction-recoiling transition points $\langle t^*/t_f\rangle$ versus the slit height h. The transition point $\langle t^*/t_f\rangle$, defined as the derivative is zero, may be fitted by a power law of h in the form of $\langle t^*/t_f\rangle = mh^n$ with m = 0.22 ± 0.04 and n = 0.2 ± 0.05 (s.e.m.).

molecule has different t_0 and t_f (= $\tau - t_0$, Figure 1g–i), and all trajectories are found to collapse at fixed l_s when the retraction time is properly rescaled (Figure 3a and Supporting Information Figure S2). The average retraction–recoil curves show close physical similarity to that observed in the squared nanochannel; the molecules elastically contract in the nano-region and then recoil outside.[35] Finding that the chain elastic

dx.doi.org/10.1021/nl2045292 | Nano Lett. 2012, 12, 1597–1602

contraction time and the recoil time are well-separated, a semi-analytical formula was proposed to account for the observed dynamics

$$l(t) = [1 + (\gamma_0 - 1)e^{-t/\tau_{el}}]\sqrt{\frac{f_{rec}}{\rho}(t_f - t)} \quad (2)$$

where ρ is the frictional drag per unit length, τ_{el} is the time scale governing the elastic chain contraction and γ_0 is the chain stretch when recoil begins. The square root term in eq 2 describes the pure entropic-recoiling motion of the molecule, whose equilibrium extension is given by $l_{rel} = \rho^{-1/2}(f_{rec}t_f)^{1/2}$ (Figure 3a).

The collapse of the average retraction trajectories (Figure 3b) suggest that eq 2 can be rewritten as

$$\left\langle \frac{l(t)}{l_s} \right\rangle = [B + (1 - B)e^{-\alpha(t/t_f)}]\sqrt{1 - \left\langle \frac{t}{t_f} \right\rangle} \quad (3)$$

where B and α are determined by fitting the collapsed curves. Supporting Information Table S1 shows that B and α are nearly independent of l_s, which supports the independence of f_{rec} on l_s, as predicted in the de Gennes[19] and Odijk[20,21] regimes. By comparison of eq 3 with eq 2, B is equivalent to l_{rel}/l_s. In addition, $l_s = a(h)(\langle t_f \rangle)^{1/2}$ since f_{rec} and ρ solely depend on h (Supporting Information Figure S4). By evaluating $a(h)$ from the experiments and B from eq 3, the recoiling force $f_{rec} = \rho B^2 a^2$ can be found once ρ is determined.

An independent measurement of ρ can be obtained from the chain mobility μ in 200 μm long slits with various h measured under an externally applied pulsed field E (Figure 3c inset). $\rho = \lambda\langle L_{nano}\rangle/\mu L_{rel}$ is determined from a linear fit of $\mu = v/E$, with v the velocity of DNA at its relaxed conformation, and the effective line charge density λ (Figure 3c).[35] However, the reported values of λ span a wide range from 0.29 e^-/nm[42,43] to 1.47 e^-/nm[9] in various systems and buffer conditions. As the experimental conditions used in ref 9 is close to ours, we adopt λ = 1.47 e^-/nm to calculate ρ (Supporting Information Figure S5) and in turn the recoiling force f_{rec}. It is noted that the scaling exponent discussed below is not affected by our choice of λ.

The transitions from elastic retraction to pure entropic recoil can be further analyzed by studying the derivative $d\langle l(t)/l_s\rangle/d\langle t/t_f\rangle$. The averaged transition time $\langle t^*/t_f\rangle$ is defined where the derivative is zero (Figure 3b, Supporting Information S3a–d) and it may be fitted by a power law of h, in the form of $\langle t^*/t_f\rangle = mh^n$, with m = 0.22 ± 0.04 and n = 0.2 ± 0.05 (s.e.m.) (Figure 3d). It indicates that $\langle t^*/t_f\rangle$ decreases as the slits become shallower, suggesting that the retraction-recoiling process is dominated by pure recoiling under strong confinement.

The values of the recoiling force in both the TOW, where $f_{rec} = -f_{el}(l_s)$, and during retracting-recoiling, where $f_{rec} = \rho B^2 a^2$, are summarized in Figure 4 and Supporting Information Table S1. During the TOW and the retracting-recoiling scenario, both forces are essentially constant irrespective of the DNA strand length inside the nanoslit and the slit length, as shown for h = 50 nm (Figure 4a). However, the scaling exponent δ ($f_{rec} \sim h^{\delta}$) obtained from the retracting–recoiling force curves is −2.8 ± 0.03 (s.e.m.), which has neither been predicted nor experimentally measured before. It is also much larger than the exponent, −0.99 ± 0.19 (s.e.m.), obtained in the TOW regime (Figure 4b). This finding points out that the value of f_{rec} depends crucially on the DNA configuration inside the slit: stretched during TOW and relaxed during the retracting–recoiling phase. On the other hand, it suggests the assumption that the DNA recoil dynamics is quasi-static needs to be re-examined, that is, the retraction–recoil dynamics needs to be sufficiently slow that the nanoconfined portion of DNA strand can be considered as in equilibrium at any time $t_0 < t < \tau$. For most single molecule force measurements of DNA using AFM, magnetic or optical tweezers, the force is applied slowly so the system is kept near equilibrium. However, the recoiling time $\langle t_f \rangle$ is found to be comparable to the elastic relaxation time of slit-confined DNA, that is, $2\tau_{el} = 2\langle t_f\rangle/\alpha$, with $\alpha \approx 4$ (see Supporting Information Table S1), and the quasi-static assumption cannot be applied. The nonequilibrium recoil dynamics that results in $f_{rec} \sim h^{-2.8}$ needs to be investigated further. On the other hand, the TOW phase can be truly considered as quasi-static. Indeed, the observed time of the TOW regime ($0 < t < t_0$ in Figure 1) is always much greater than $2\langle t_f\rangle/\alpha$, and the corresponding recoiling force measurements may be considered as in equilibrium.

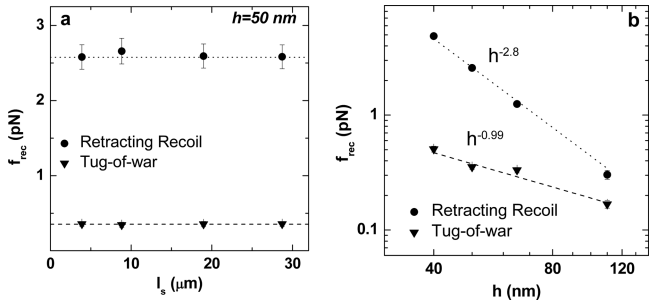

Figure 4. Recoiling force analysis. (a) Entropic recoiling force f_{rec} versus l_s under retracting recoil (●) and TOW (▼) regimes for h = 50 nm. Dotted lines stand for the averages over different l_s. (b) Log–log plot of entropic recoiling force f_{rec} versus h for DNA TOW and retracting recoiling. Dashed lines are the best fit ($f_{rec} \sim h^{\delta}$) of the experimental values and yield the corresponding scaling exponents δ = −0.99 ± 0.19 (s.e.m.) and −2.8 ± 0.03 (s.e.m.) for the TOW and the retracting recoiling regime, respectively.

Finally, it may be of interest to compare our system to that of an optical or magnetic tweezers-based system. The range of the recoiling force exerted by the entropy difference at micro–nano interfaces in our system is mainly determined by the confinement from the slit height h and the resolution by how fine we can vary h while maintaining the force difference experimentally resolvable. On the other hand, a tweezers-based system could exert a force with better resolution and wider range, particularly in the force range larger than a pN. It is also suitable to study the force–extension relation in the lesser-confined de Gennes regime where the entropic difference caused by micro–nano interface is minimal and hence a TOW scenario could be hard to set up as discussed earlier. Although it is challenging to integrate a tweezers-based system into a fluidic device with micro–nano interfaces, it has recently been demonstrated with the controllability of band-passing certain elastic modes of a biopolymer.[44]

In summary, we established entropically trapped extension of single DNA molecules during the TOW scenario, in which single DNA molecules straddle across a nanoslit bridging two micro-nanofluidic interfaces. This scheme allows us to study the scaling relations that govern both the TOW regime and confinement-induced entropic recoiling at various slit lengths and heights. In both equilibrium (tug-of-war) and nonequilibrium (retracting-recoiling) phases, the recoiling force is shown to be constant for a given degree of confinement, irrespective of the DNA length inside the nanoslit and the slit length, which is in agreement with

dx.doi.org/10.1021/nl2045292 | Nano Lett. 2012, 12, 1597–1602

the prediction of polymer theory. In the TOW regime, the recoiling force dependence on the slit depth is found to be $f_{rec} \sim h^{-1}$. This agrees with the scaling theory prediction of a highly stretched polymer chain confined in a nanoslit in both the de Gennes and the Odijk regimes. We note that this finding is consistent with the recent measurements of equilibrium diffusivity and relaxation time in strongly confined chains in slit,[28,45] which did not find any dramatic crossover from $h > P$ to $h < P$. In the retracting-recoiling regime, the scaling is found to be $f_{rec} \sim h^{-2.8}$, where the normalized transition time from retraction to recoil follows a power law, $\langle t^*/t_f \rangle = 0.22h^{0.2}$. These observations are novel and remain to be tested by theory and simulations. Overall, our findings may help elucidate the single polymer dynamics at micro−nanoscale interfaces and pave the way to study fluctuation-induced polymer translocation in artificial or biological nanopore systems. We expect the scaling analysis presented here may stimulate further theoretical and experimental works and have implications to device design for single molecule analysis and biotechnological applications.

■ ASSOCIATED CONTENT

Ⓢ Supporting Information

Detailed description of the quasi-static model for DNA tug-of-war, modified wormlike chain force−extension relation, and experimental methods. Five additional figures (Figures S1−S5) on the Brownian dynamics simulation, scaling analysis, elastic-recoiling transition, and so forth along with a table summarizing the recoiling force analysis and a movie demonstrating the single DNA tug-of-war and its retracting-recoil process. This material is available free of charge via the Internet at http://pubs.acs.org.

■ AUTHOR INFORMATION

Corresponding Author

*E-mail: cfchou@phys.sinica.edu.tw.

Present Address

[#]CNR-IENI, Milano, Italy.

Author Contributions

[¶]These authors contributed equally to this work.

Notes

The authors declare no competing financial interest.

■ ACKNOWLEDGMENTS

We thank Jie-Pan Shen for his early involvement in this project. We are grateful to Professors Walter Reisner and Tom Perkins for their critical review of the manuscript and insightful suggestions, to Yi-Ren Chang and Yii-Lih Lin for bulk persistence length measurements, and to Professors Masao Doi, C. C. Huang, Chih-Chen Hsieh, Wokyung Sung, Derek Stein, and Helmut Schlessel for helpful discussions. This research was supported by Stanford University (CIS Grant 1092418-1-EALGD), Academia Sinica Program on Nanotechnology and the Foresight Project AS-97-FP-M02 (to C.F.C.), AS Postdoctoral Fellowship (to A.T.) and by National Science Council (ROC) 98-2112-M-001-004-MY3 (to Y.L.C.), 96-2112-M-001-024-MY3, and 99-2112-M-001-027-MY3 (to C.F.C.). Work was performed in part at the Stanford Nanofabrication Facility of NNIN supported by NSF ECS-9731293 and at the AS Nano Core Facilities. C.F.C. conceived the experiments. C.F.C. and J.W.Y. designed the experiments. J.W.Y. fabricated the devices and performed the experiments. A.T. and Y.L.C. contributed to the modified wormlike chain model. Y.L.C. performed the Brownian dynamics simulations (yenglong@phys.sinica.edu.tw). A.T. derived the quasi-static model for DNA tug-of-war and the retraction-recoiling curves rescaling. J.W.Y. and A.T. analyzed the data. J.W.Y., A.T., Y.L.C., and C.F.C. co-wrote the paper.

■ REFERENCES

(1) Bakajin, O. B.; Duke, T. A. J.; Chou, C. F.; Chan, S. S.; Austin, R. H.; Cox, E. C. *Phys. Rev. Lett.* **1998**, *80*, 2737−2740.
(2) Han, J.; Turner, S. W.; Craighead, H. G. *Phys. Rev. Lett.* **1999**, *83*, 1688−1691.
(3) Smith, D. E.; Tans, S. J.; Smith, S. B.; Grimes, S.; Anderson, D. L.; Bustamante, C. *Nature* **2001**, *413*, 748−752.
(4) Turner, S. W. P.; Cabodi, M.; Craighead, H. G. *Phys. Rev. Lett.* **2002**, *88*, 128103.
(5) Tegenfeldt, J. O.; Prinz, C.; Cao, H.; Chou, S.; Reisner, W. W.; Riehn, R.; Wang, Y. M.; Cox, E. C.; Sturm, J. C.; Silberzan, P.; Austin, R. H. *Proc. Natl. Acad. Sci. U.S.A.* **2004**, *101*, 10979−10983.
(6) Reisner, W.; Larsen, N. B.; Flyvbjerg, H.; Tegenfeldt, J. O.; Kristensen, A. *Proc. Natl. Acad. Sci. U.S.A.* **2009**, *106*, 79−84.
(7) Muthukumar, M. *Phys. Rev. Lett.* **2001**, *86*, 3188−3191.
(8) Chen, P.; Mitsui, T.; Farmer, D. B.; Golovchenko, J.; Gordon, R. G.; Branton, D. *Nano Lett.* **2004**, *4*, 1333−1337.
(9) Keyser, U. F.; Koeleman, B. N.; Van Dorp, S.; Krapf, D.; Smeets, R. M. M.; Lemay, S. G.; Dekker, N. H.; Dekker, C. *Nat. Phys.* **2006**, *2*, 473−477.
(10) van Dorp, S.; Keyser, U. F.; Dekker, N. H.; Dekker, C.; Lemay, S. G. *Nat. Phys.* **2009**, *5*, 347−351.
(11) Gauthier, M. G.; Slater, G. W. *Eur. Phys. J. E* **2008**, *25*, 17−23.
(12) de Haan, H.; Slater, G. *Phys. Rev. E* **2010**, *81*, 051802.
(13) Han, J.; Craighead, H. G. *Science* **2000**, *288*, 1026−1029.
(14) Wang, Y. C.; Stevens, A. L.; Han, J. Y. *Anal. Chem.* **2005**, *77*, 4293−4299.
(15) Pu, Q. S.; Yun, J. S.; Temkin, H.; Liu, S. R. *Nano Lett.* **2004**, *4*, 1099−1103.
(16) Holt, J. K.; Park, H. G.; Wang, Y. M.; Stadermann, M.; Artyukhin, A. B.; Grigoropoulos, C. P.; Noy, A.; Bakajin, O. *Science* **2006**, *312*, 1034−1037.
(17) Sparreboom, W.; van den Berg, A.; Eijkel, J. C. T. *Nat. Nanotechnol.* **2009**, *4*, 713−720.
(18) Dorfman, K. D. *Rev. Mod. Phys.* **2010**, *82*, 2903−2947.
(19) Gennes, P.-G. d. *Scaling Concepts in Polymer Physics;* Cornell University Press: Ithaca, NY, 1979.
(20) Odijk, T. *Macromolecules* **1995**, *28*, 7016−7018.
(21) Burkhardt, T. W. *J. Phys. A* **1997**, *30*, L167−L172.
(22) Odijk, T. *Phys. Rev. E* **2008**, *77*, 060901.
(23) Reisner, W.; Morton, K. J.; Riehn, R.; Wang, Y. M.; Yu, Z. N.; Rosen, M.; Sturm, J. C.; Chou, S. Y.; Frey, E.; Austin, R. H. *Phys. Rev. Lett.* **2005**, *94*, 196101.
(24) Hsieh, C.-C.; Balducci, A.; Doyle, P. S. *Macromolecules* **2007**, *40*, 5196.
(25) Hsieh, C.-C.; Balducci, A.; Doyle, P. S. *Nano Lett.* **2008**, *8*, 1683−1688.
(26) Strychalski, E. A.; Levy, S. L.; Craighead, H. G. *Macromolecules* **2008**, *41*, 7716−7721.
(27) Underhill, P. T.; Doyle, P. S. *J. Rheol.* **2006**, *50*, 513−529.
(28) Lin, P. K.; Fu, C. C.; Chen, Y. L.; Chen, Y. R.; Wei, P. K.; Kuan, C. H.; Fann, W. S. *Phys. Rev. E* **2007**, *76*, 011806.
(29) Lin, P. K.; Lin, K. H.; Fu, C. C.; Lee, K. C.; Wei, P. K.; Pai, W. W.; Tsao, P. H.; Chen, Y. L.; Fann, W. S. *Macromolecules* **2009**, *42*, 1770−1774.
(30) Lin, P.-K.; Chang, J.-F.; Wei, C.-H.; Tsao, P. H.; Fann, W. S.; Chen, Y.-L. *Phys. Rev. E* **2011**, *84*, 031917.
(31) Bonthuis, D. J.; Meyer, C.; Stein, D.; Dekker, C. *Phys. Rev. Lett.* **2008**, *101*, 108303.
(32) Bustamante, C.; Marko, J. F.; Siggia, E. D.; Smith, S. *Science* **1994**, *265*, 1599−1600.
(33) Perkins, T. T.; Quake, S. R.; Smith, D. E.; Chu, S. *Science* **1994**, *264*, 822−826.

(34) Neuman, K. C.; Nagy, A. *Nat. Methods* **2008**, *5*, 491−505.
(35) Mannion, J. T.; Reccius, C. H.; Cross, J. D.; Craighead, H. G. *Biophys. J.* **2006**, *90*, 4538−4545.
(36) Gu, J.; Gupta, R.; Chou, C. F.; Wei, Q. H.; Zenhausern, F. *Lab Chip* **2007**, *7*, 1198−1201.
(37) Guo, L. J.; Cheng, X.; Chou, C. F. *Nano Lett.* **2004**, *4*, 69−73.
(38) Chuang, J.; Kantor, Y.; Kardar, M. *Phys. Rev. E* **2002**, *65*, 011802.
(39) Zoia, A.; Rosso, A.; Majumdar, S. N. *Phys. Rev. Lett.* **2009**, *102*, 120602.
(40) Marko, J. F.; Siggia, E. D. *Macromolecules* **1995**, *28*, 8759−8770.
(41) Chen, Y. L.; Lin, P. K.; Chou, C. F. *Macromolecules* **2010**, *43*, 10204−10207.
(42) Gurrieri, S.; Smith, S. B.; Bustamante, C. *Proc. Natl. Acad. Sci. U.S.A.* **1999**, *96*, 453−458.
(43) Smith, S. B. *Biopolymers* **1990**, *29*, 1167−1173.
(44) Lin, J.; Persson, F.; Fritzsche, J.; Tegenfeldt, J. O.; Saleh, O. A. *Biophys. J.* **2012**, *102*, 96−100.
(45) Tang, J.; Levy, S. L.; Trahan, D. W.; Jones, J. J.; Craighead, H. G.; Doyle, P. S. *Macromolecules* **2010**, *43*, 7368−7377.